Supporting information for:

Functional traits and metacommunity theory reveal that habitat filtering and competition maintain bird diversity in a human-shared landscape

Harold N. Eyster[1,2,3*], Diane S. Srivastava[2,4], Maayan Kreitzman[1,2], and Kai M. A. Chan[1,2]

[1]Institute for Resources, Environment and Sustainability, University of British Columbia, Canada
[2]Biodiversity Research Centre, University of British Columbia, Canada
[3]Gund Institute for Environment, University of Vermont, Burlington, VT, USA
[4]Department of Zoology, University of British Columbia, Canada

*Corresponding author. Please direct any questions or comments to haroldeyster@gmail.com.

1 Additional methods

1.1 Number of point counts at each farm

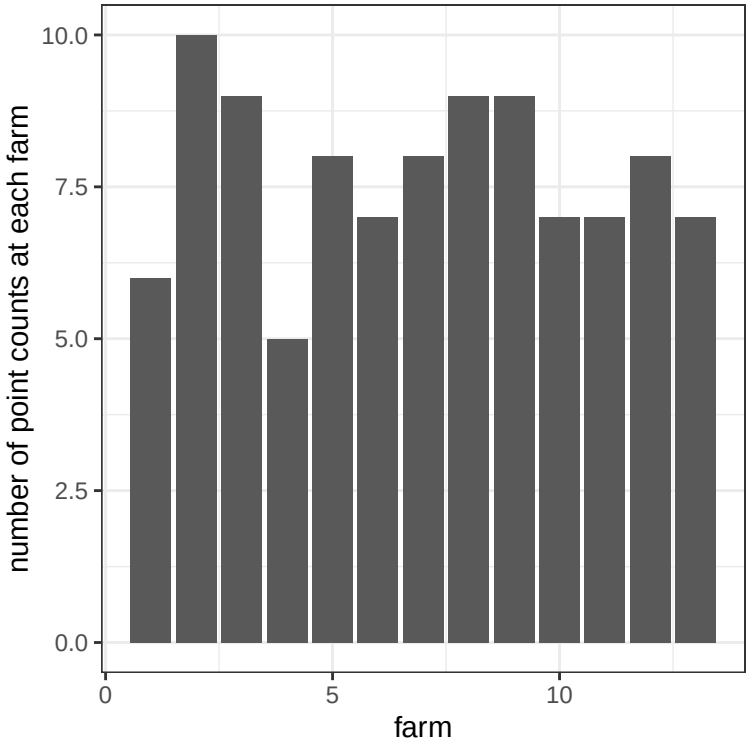

1.2 Woods and prairie habitat details

Woods in the southern part of our study region are dominated by secondary temperate broad-leaf deciduous trees, including *Fraxinus*, *Quercus*, *Acer*, *Junglans*, *Gleditsia triacanthos*, *Celtus*, and *Carya*, while northern part is dominated by coniferous and broad-leaf trees, including *Betula*, *Pinus*, *Populus*, *Acer*, *Fagus*, and *Tsuga*. Prairies are dominated by native grasses (e.g., *Andropogon gerardii*, *Schizachyrium scoparium*), invasive grasses (especially *Phalaris arundinacea*), and forbs, particularly *Solidago*, and *Aster*.

1.3 Additional model details

N-mixture models require that count data be temporally replicated and that populations be effectively closed (Kéry et al., 2005, i.e., recruitment, survival, immigration, and emigration must be negligible). Our data satisfy these assumptions because our counts were all replicated within two days of each other and occurred in the breeding season (when birds are quite sedentary). We removed flyovers that did not use the habitat and nocturnal owls, since we did not target nocturnal species in our survey.

The likelihood function for these models presents an identifiability issue, whereby $p = 0$ is a local maximum, yielding an infinite estimate of λ (Dennis et al., 2015). This issue occurs when the covariance between detection on different sampling occasions is greater than zero

(Dennis et al., 2015). This issue is especially likely when the number of temporal replicates is small (as in our case). We overcame this issue by using priors on the detection probability (N(0.8,0.1)) and an upper constraint, K, on the true number of individuals present at a point count (Royle, 2004). We used a value of K = 80; this was nearly double the largest number of individuals seen at a single point count, and it is highly unlikely that any species had this many individuals in a single 50-m radius count circle. All other parameters were given weakly informative normally distributed priors. To make the model geometry easier to sample, we performed non-centered reparameterizations (Betancourt & Girolami, 2015) of habitat, cluster, and detection variables (Carpenter, 2016).

N-Mixture models are typically built with the BUGS family of languages, which use Metropolis-Hastings algorithms. However, these algorithms struggle to recover the mode from high-dimensional models (due to 'concentration of measure,' see McElreath, 2020). The Stan probabilistic programming language (Carpenter et al., 2017) overcomes this challenge by using a more efficient sampling algorithm (Hamiltonian Monte Carlo no-U-turn sampler; Hoffman & Gelman, 2014). Stan also provides diagnostics that signal when the posterior has not been accurately explored. Thus we used Stan to build our multispecies N-mixture abundance model; to our knowledge, our model is the first example of Stan being used to build a multispecies abundance model.

1.4 Brown-headed Cowbird lifehistory traits

Data on Brown-headed Cowbird (*Molothrus ater*, an obligate brood parasite) traits were absent from Tobias and Pigot (2019) and instead taken from Lowther (2020). Clutch size was estimated by calculating the geometric mean of the minimum and maximum reported clutch sizes (following Jetz et al., 2008).

1.5 Functional trait dimension reduction

To account for collinearity between traits, we conducted a principal component analysis (PCA) on all 34 traits (both categorical and continuous traits) using the `FactoMineR` package in `R` (Lê et al., 2008). To determine which of the resulting dimensions were stable and likely to represent true trait structure, we performed a bootstrap resampling analysis, following Pillar (1999). This analysis entailed taking 500 bootstrapped samples (with replacement) from the trait matrix. Next we performed a PCA on each bootstrapped sample, and calculated the correlation between the resultant bootstrap PCA values and the values from the original trait matrix (note that before estimating the correlation, we conducted a Procrustean dilation, translation, and rotation (Schönemann & Carroll, 1970) of the bootstrapped PCA values to make them comparable with the original PCA values). We then conducted an identical exercise, except with a trait matrix that had been randomly permuted within traits. Finally, we compared the correlations produced by these two pipelines, and produced a p-value that reveals which dimensions stably represent synthetic trait structure. We repeated this analysis for each number of dimensions, up to 34 (see details in Pillar, 1999). This method suggested that the first dimension was highly significant (p=0.002), the second was marginal (p=0.1); additional dimensions were highly non-significant (p >0.3). Furthermore, the first two dimensions were ecologically interpretable (relating to size, diet, and foraging/singing

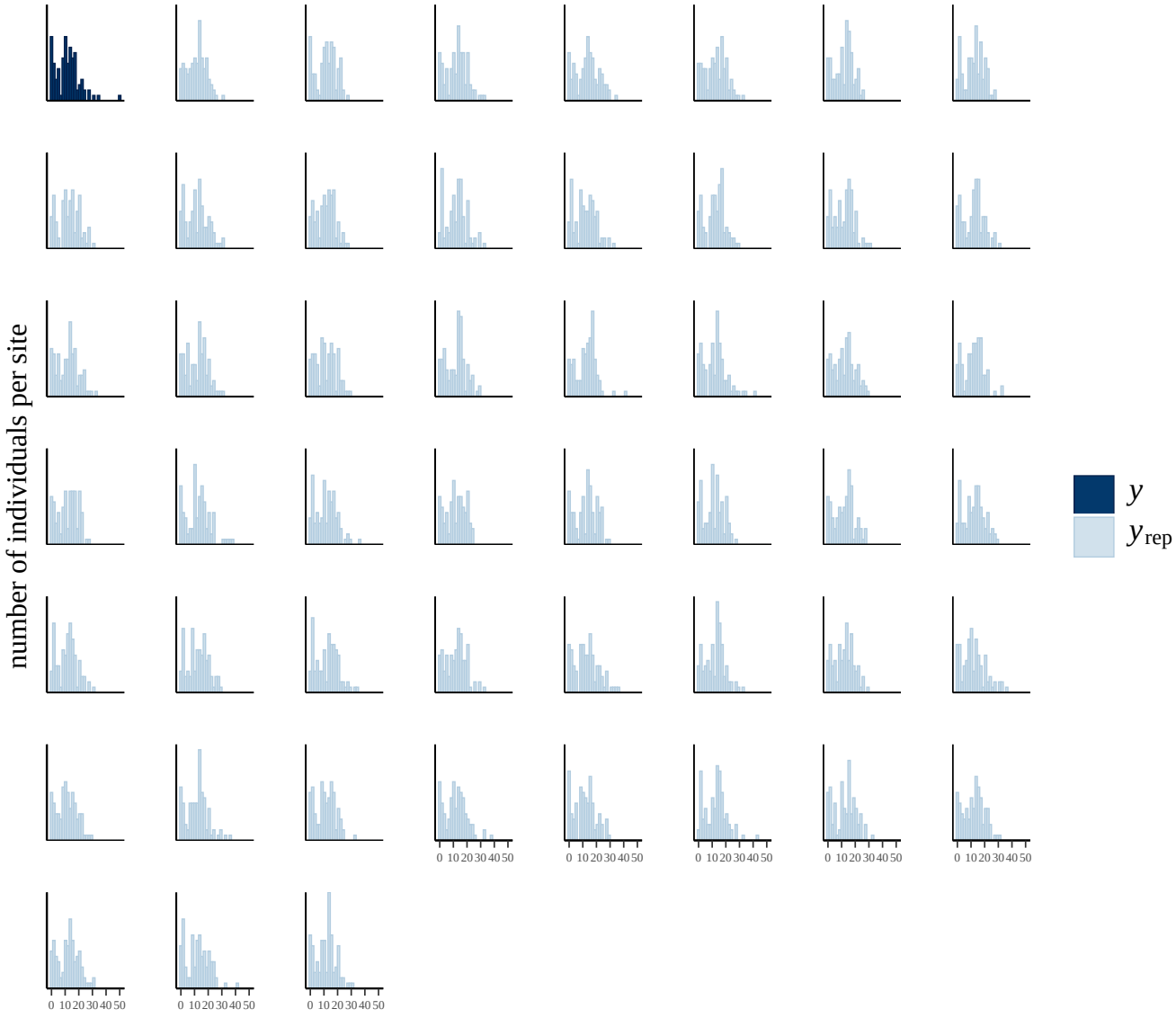

Figure S1: Posterior predictive checks showing the actual number of individuals observed at each site and 50 draws from the posterior predictive distribution.

strata: see Figure 3). Thus, all further analyses used the first two trait dimensions to represent functional traits.

1.6 Metacommunity process analysis

We investigated relationships between the local environment and functional traits to elucidate which assembly processes drive bird diversity. If the functional traits expressed in a given community are unrelated to the environment, then stochasticity and/or dispersal likely drive diversity. However, if each environment is associated with a different set of convergent traits, then filtering likely drives diversity. On the other hand, if an environmental gradient is associated with trait divergence, then competition likely drives diversity. Importantly, competition and filtering can both be significant for a given metacommunity (Ingram & Shurin, 2009). For example, some traits may respond to competition (i.e., alpha-niche traits) while others respond to filtering (i.e., beta-niche traits; Leibold & Chase, 2017). However, because these two processes lead to opposing patterns, one can cancel the signal of the other (which can be exacerbated when traits are analyzed simultaneously). Thus, for every individual trait axis, we looked for signs of competition (trait divergence assembly patterns; TDAP; Pillar, 1999; Stubs & Wilson, 2004) and competition (trait convergence assembly patterns; TCAP) using a method that independently estimates the importance of each process (Pillar & d. S. Duarte, 2010; Pillar et al., 2009). We conducted this analysis separately at two environmental scales: local (across habitats) and regional (across clusters).

To identify trait convergence assembly patterns (signaling filtering) we compared how well the environmental gradient matched the functional trait gradient. More precisely, we computed the trait–community matrix by multiplying the trait–species matrix by the species–community matrix. Next we computed Euclidean distance matrices using the trait–community matrix and the environment–community matrix. We then calculated the partial correlation between these two distance matrices (ρTE, Pillar et al., 2009), which represents the congruence between the environmental gradient and the trait gradient, thereby signaling the presence of filtering.

To identify trait divergence assembly patterns (signaling competition) we first used the species–trait matrix to classify each species into fuzzy types. This new type–species matrix signifies how well each species fits into each type. We then repeated the same method as for trait convergence, except using the type–species matrix instead of the trait–species matrix. By using this type–species matrix, we are able to identify both trait convergence and trait divergence patterns. For example, if a community in a cold environment contains species with moderate trait values, while a community in a hot environment contains species with both low and high trait values, these communities exhibit trait divergence. Using the original trait–species matrix, these communities would not appear to vary with temperature. But using the type–species matrix, we are able to see that the cold environment has species in one type, while the hot environment contains species in two other types (for details and examples, see Pillar et al., 2009). This trait-to-type transformation effectively turns continuous trait variables into factor variables. However, using the type–species matrix reveals both trait convergence and trait divergence patterns. To isolate trait divergence pattern ($\rho XE.T$) we effectively removed any sign of trait convergence (as estimated using the trait–species matrix; for details, see Pillar et al., 2009).

1.7 Perennial crops

Table S1: Perennial crops grown in each of the perennial polyculture farms included in this study

farm˙no.	perennial˙crops
1	Chestnut, plum, blackberry, black currants, sugar maple, witch hazel, winterberry
2	Chestnut, hazelnut, red currants, black currants, rhubarb
3	Chestnut, pawpaw, gooseberry, black currant, comfrey, persimon, Asian pear, heartnut, blackberry
4	Chestnut, hazelnut, persimmon, pawpaw
5	Chestnut, persimmon, cherry, apple, seaberry, pawpaw, honeyberry, elderberry, hawthorne, apricot, hay in some alleys
6	Hazelnut, blackberry, red currant, black currant, chestnut, apple, saskatoon berry, raspberry, rhubarb, hay in some alleys
7	Plum, persimmon, cherry, quince, ash, pear, blackberry, rose, black currant, gooseberry, aronia
8	Chestnut, gooseberry, black currant, red currant, mulberry, elderberry, apple, hazelnut
9	Apple, quince, black currant, aronia, saskatoon berry, seaberry, elderberry, apricot, crabapple, asian pear, plum, chives
10	Hazelnut, elderberry, corn and sunflower and clover in alleys
12	Apple, pear, grape, saskatoon berries, red currant, black currant, gooseberries, plum, apricot, highbush cranberry, aronia, blueberry, honeyberry, garlic
13	Apple, plum, black currant, apricot, cherry, clover in alleys, various flowers
14	Pear, apple, highbush cranberry, elderberry, linden

1.8 Bird species codes

Our original data and some supplementary figures use four-letter alpha codes from the Institute for Bird Populations to refer to each species, according to the following table:

Table S2: Alpha codes, common names, and new and old scientific names for each bird species included in this study

IBP˙code	common˙name	scientific˙name	old˙scientific˙name
ALFL	Alder Flycatcher	Empidonax alnorum	Empidonax alnorum
AMCR	American Crow	Corvus brachyrhynchos	Corvus brachyrhynchos
AMGO	American Goldfinch	Spinus tristis	Carduelis tristis
AMRE	American Redstart	Setophaga ruticilla	Setophaga ruticilla
AMRO	American Robin	Turdus migratorius	Turdus migratorius
BANS	Bank Swallow	Riparia riparia	Riparia riparia
BAOR	Baltimore Oriole	Icterus galbula	Icterus galbula
BARS	Barn Swallow	Hirundo rustica	Hirundo rustica
BBCU	Black-billed Cuckoo	Coccyzus erythropthalmus	Coccyzus erythropthalmus
BCCH	Black-capped Chickadee	Poecile atricapillus	Parus atricapillus
BEVI	Bell's Vireo	Vireo bellii	Vireo bellii
BGGN	Blue-gray Gnatcatcher	Polioptila caerulea	Polioptila caerulea
BHCO	Brown-headed Cowbird	Molothrus ater	Molothrus ater
BLGR	Blue Grosbeak	Passerina caerulea	Passerina caerulea
BLJA	Blue Jay	Cyanocitta cristata	Cyanocitta cristata
BOBO	Bobolink	Dolichonyx oryzivorus	Dolichonyx oryzivorus
NOBO	Northern Bobwhite	Colinus virginianus	Colinus virginianus
BRTH	Brown Thrasher	Toxostoma rufum	Toxostoma rufum
CACH	Carolina Chickadee	Poecile carolinensis	Parus carolinensis
CARW	Carolina Wren	Thryothorus ludovicianus	Thryothorus ludovicianus
CCSP	Clay-colored Sparrow	Spizella pallida	Spizella pallida
CEDW	Cedar Waxwing	Bombycilla cedrorum	Bombycilla cedrorum
CHSP	Chipping Sparrow	Spizella passerina	Spizella passerina
CLSW	Cliff Swallow	Petrochelidon pyrrhonota	Petrochelidon pyrrhonota
COGR	Common Grackle	Quiscalus quiscula	Quiscalus quiscula
CORA	Common Raven	Corvus corax	Corvus corax
COYE	Common Yellowthroat	Geothlypis trichas	Geothlypis trichas
DICK	Dickcissel	Spiza americana	Spiza americana
DOWO	Downy Woodpecker	Dryobates pubescens	Picoides pubescens
EABL	Eastern Bluebird	Sialia sialis	Sialia sialis
EAKI	Eastern Kingbird	Tyrannus tyrannus	Tyrannus tyrannus
EAME	Eastern Meadowlark	Sturnella magna	Sturnella magna
EAPH	Eastern Phoebe	Sayornis phoebe	Sayornis phoebe
EATO	Eastern Towhee	Pipilo erythrophthalmus	Pipilo erythrophthalmus
EAWP	Eastern Wood-pewee	Contopus virens	Contopus virens
EUST	European Starling	Sturnus vulgaris	Sturnus vulgaris
FISP	Field Sparrow	Spizella pusilla	Spizella pusilla
GCFL	Golden-crowned Kinglet	Regulus satrapa	Regulus satrapa
GRCA	Gray Catbird	Dumetella carolinensis	Dumetella carolinensis
HAWO	Hairy Woodpecker	Dryobates villosus	Picoides villosus
HESP	Henslow's Sparrow	Centronyx henslowii	Ammodramus henslowii
HOLA	Horned Lark	Eremophila alpestris	Eremophila alpestris
HOSP	House Sparrow	Passer domesticus	Passer domesticus
HOWR	House Wren	Troglodytes aedon	Troglodytes aedon
INBU	Indigo Bunting	Passerina cyanea	Passerina cyanea
LASP	Lark Sparrow	Chondestes grammacus	Chondestes grammacus
LEFL	Least Flycatcher	Empidonax minimus	Empidonax minimus
LISP	Lincoln's Sparrow	Melospiza lincolnii	Melospiza lincolnii
MODO	Mourning Dove	Zenaida macroura	Zenaida macroura
NOCA	Northern Cardinal	Cardinalis cardinalis	Cardinalis cardinalis
OROR	Orchard Oriole	Icterus spurius	Icterus spurius
OVEN	Ovenbird	Seiurus aurocapilla	Seiurus aurocapilla
PIGR	Pine Grosbeak	Pinicola enucleator	Pinicola enucleator
RBGR	Rose-breasted Grosbeak	Pheucticus ludovicianus	Pheucticus ludovicianus
RBNU	Red-breasted Nuthatch	Sitta canadensis	Sitta canadensis
RBWO	Red-bellied Woodpecker	Melanerpes carolinus	Melanerpes carolinus
REVI	Red-eyed Vireo	Vireo olivaceus	Vireo olivaceus
RHWO	Red-headed Woodpecker	Melanerpes erythrocephalus	Melanerpes erythrocephalus
RNPH	Ring-necked Pheasant	Phasianus colchicus	Phasianus colchicus
RTHU	Ruby-throated Hummingbird	Archilochus colubris	Archilochus colubris
RWBL	Red-winged Blackbird	Agelaius phoeniceus	Agelaius phoeniceus
SAVS	Savannah Sparrow	Passerculus sandwichensis	Passerculus sandwichensis
SCTA	Scarlet Tanager	Piranga olivacea	Piranga olivacea
SEWR	Sedge Wren	Cistothorus platensis	Cistothorus platensis
SOSP	Song Sparrow	Melospiza melodia	Melospiza melodia
TUTI	Tufted Titmouse	Baeolophus bicolor	Baeolophus bicolor
VESP	Vesper Sparrow	Pooecetes gramineus	Pooecetes gramineus
WAVI	Warbling Vireo	Vireo gilvus	Vireo gilvus
WBNU	White-breasted Nuthatch	Sitta carolinensis	Sitta carolinensis
WIFL	Willow Flycatcher	Empidonax traillii	Empidonax traillii
WITU	Wild Turkey	Meleagris gallopavo	Meleagris gallopavo
WOTH	Wood Thrush	Hylocichla mustelina	Hylocichla mustelina
YBCH	Yellow-breasted Chat	Icteria virens	Icteria virens
YBCU	Yellow-billed Cuckoo	Coccyzus americanus	Coccyzus americanus
YBSA	Yellow-bellied Sapsucker	Sphyrapicus varius	Sphyrapicus varius
YEWA	Yellow Warbler	Setophaga petechia	Dendroica petechia
YSFL	Northern Flicker	Colaptes auratus	Colaptes auratus
YTVI	Yellow-throated Vireo	Vireo flavifrons	Vireo flavifrons

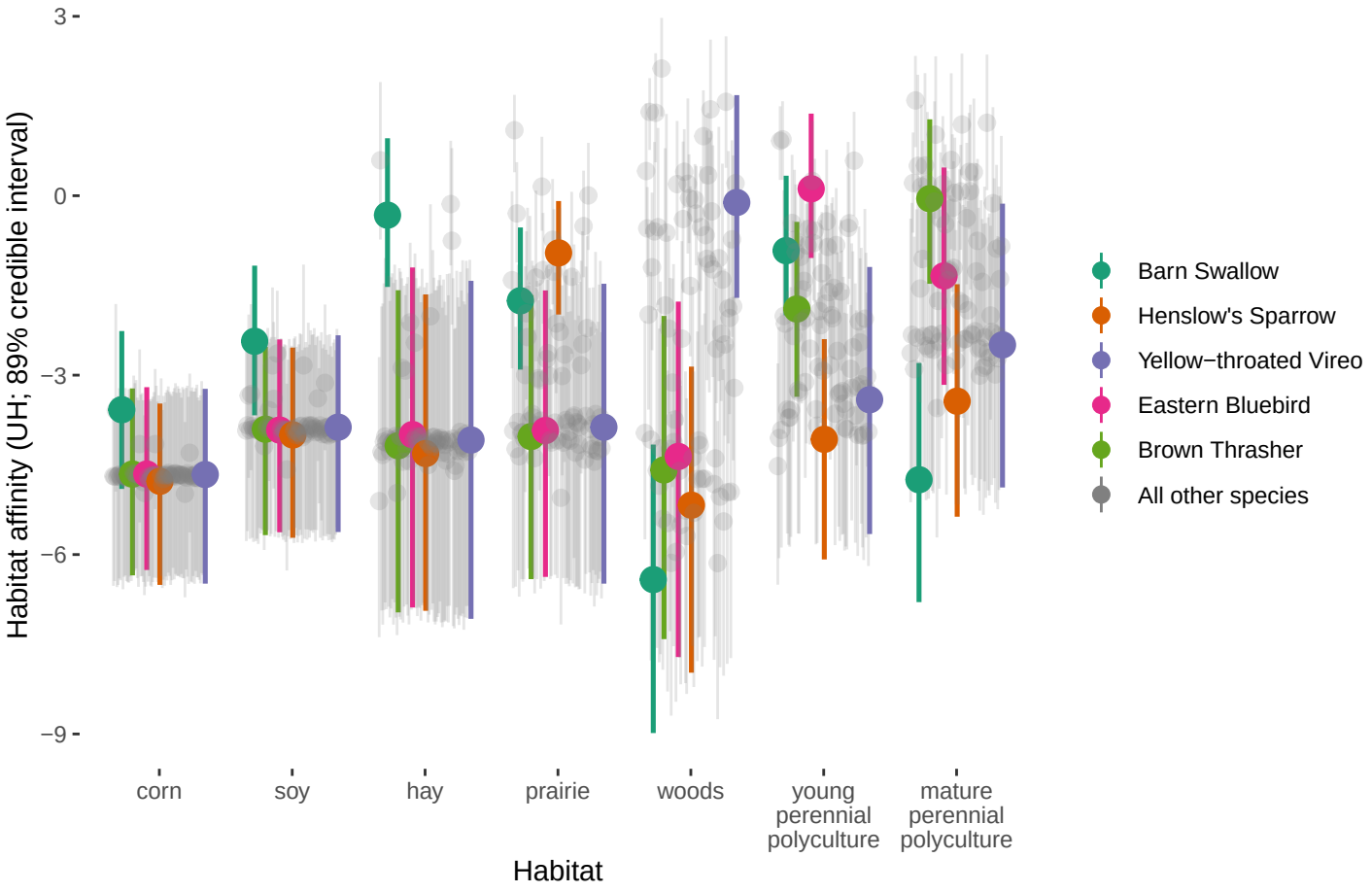

Figure S2: Replicate of Figure 2, but with 89% credible intervals.

2 Results

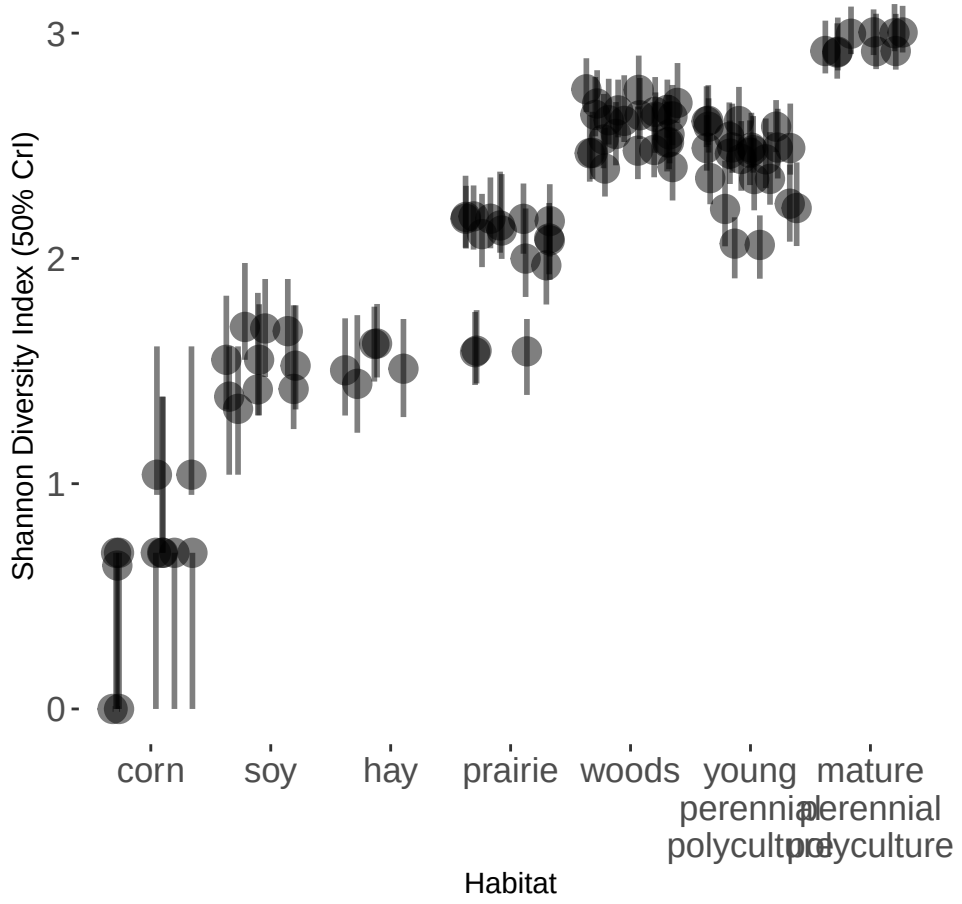

Figure S3: Predicted Shannon Diversity Index at each sampling point. Bars represent 50% credible intervals.

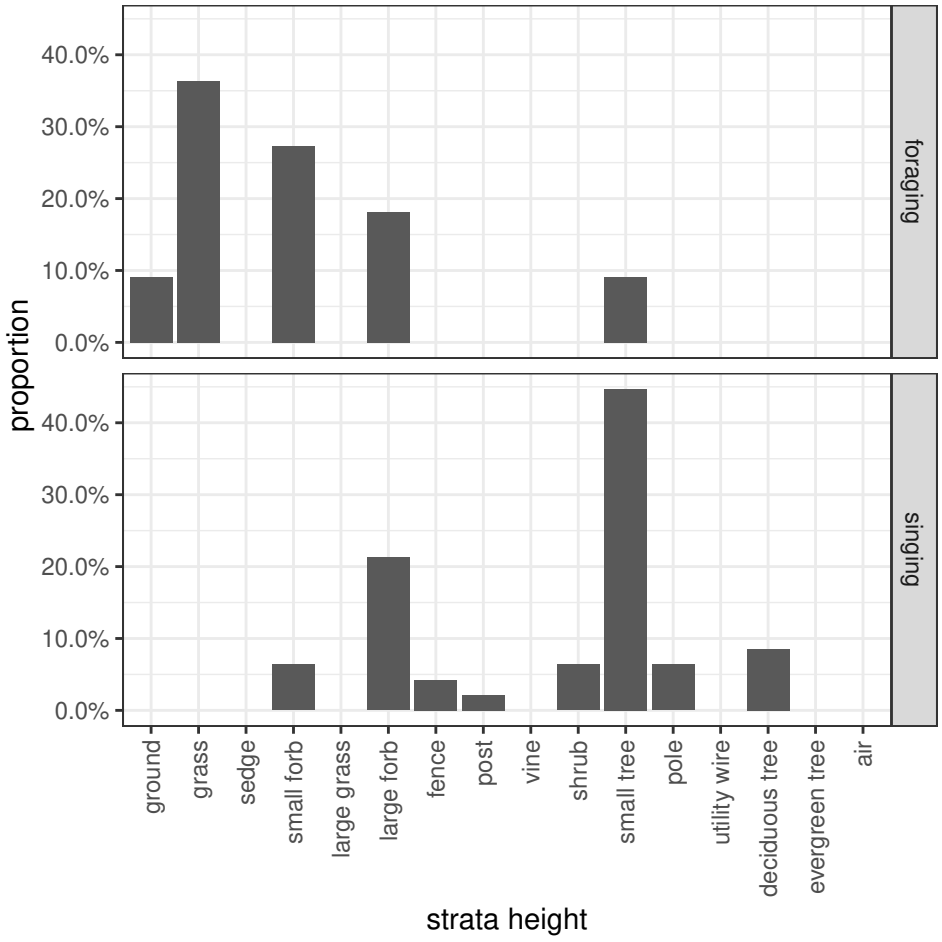

Figure S4: Observed singing vs. foraging strata of Dickcissel (*Spiza americana*).

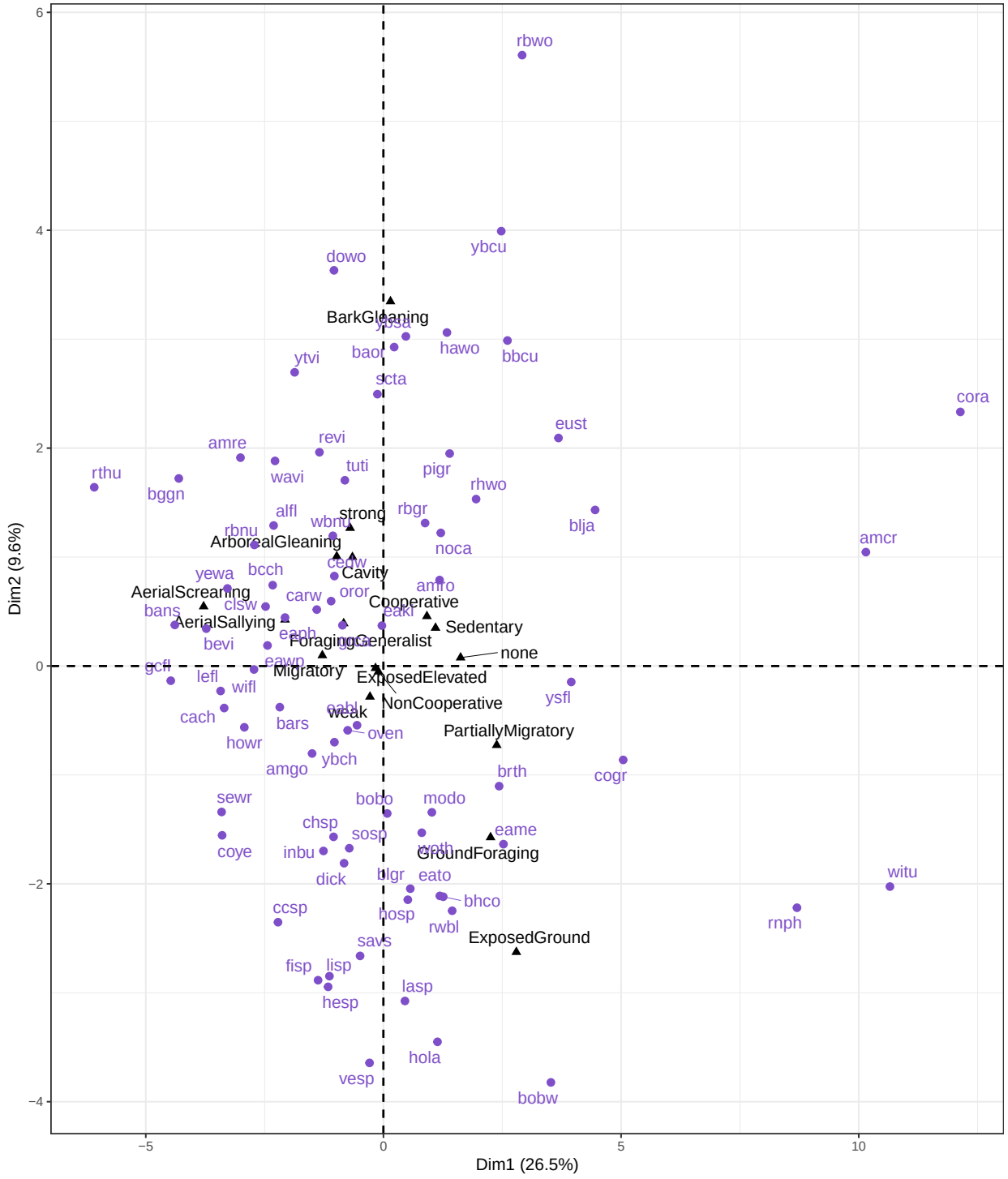

Figure S5: Principal components analysis (PCA) ordination of bird species on the two trait dimensions. For functional trait abbreviation legend, see Table 1. For bird species codes, see Table S2.

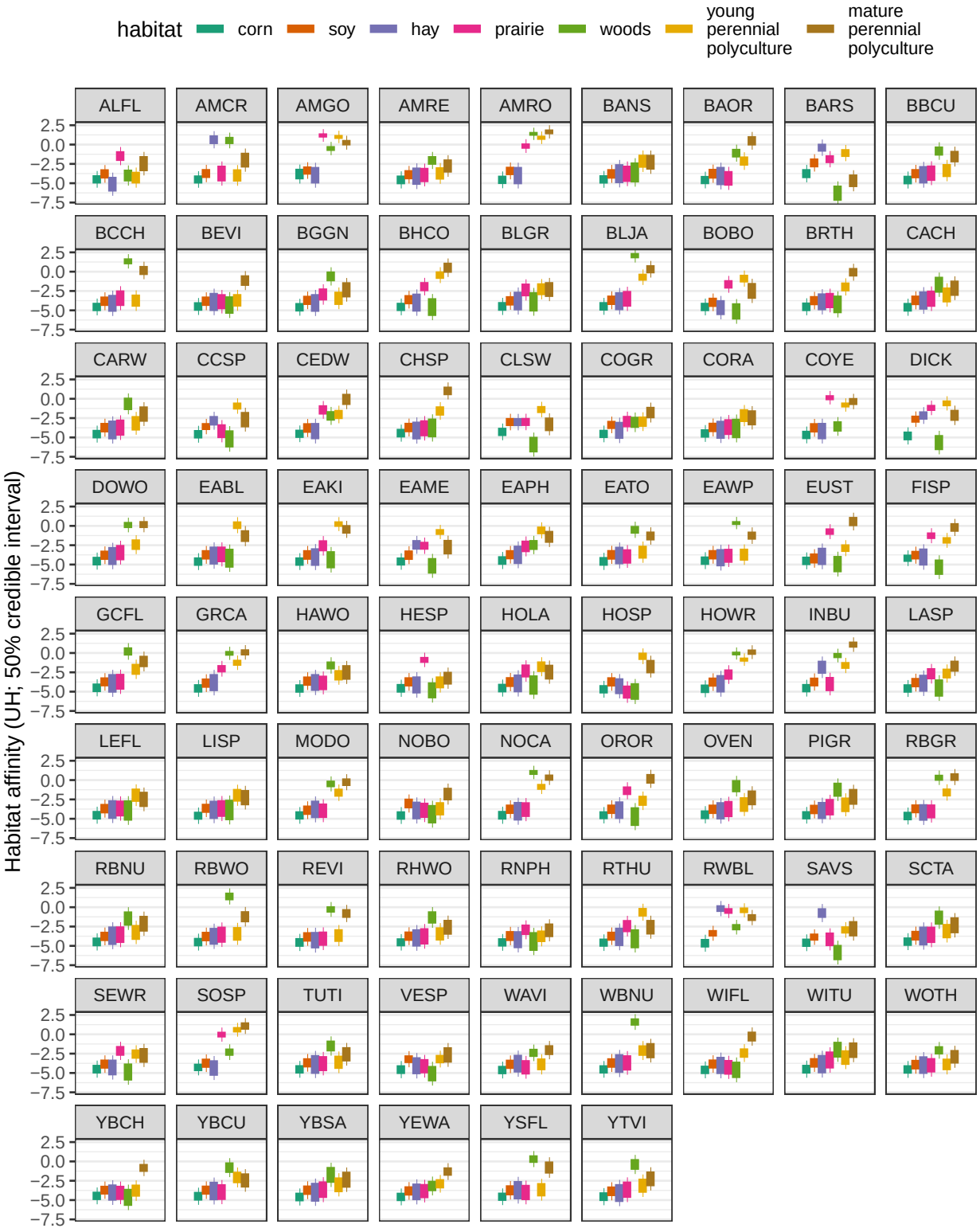

Figure S6: Model estimates of each species' affinity for each habitat type, showing each species separately. These estimates control for the effect of site cluster, in order to show only the effect of habitat type. Bars represent 50% credible intervals.

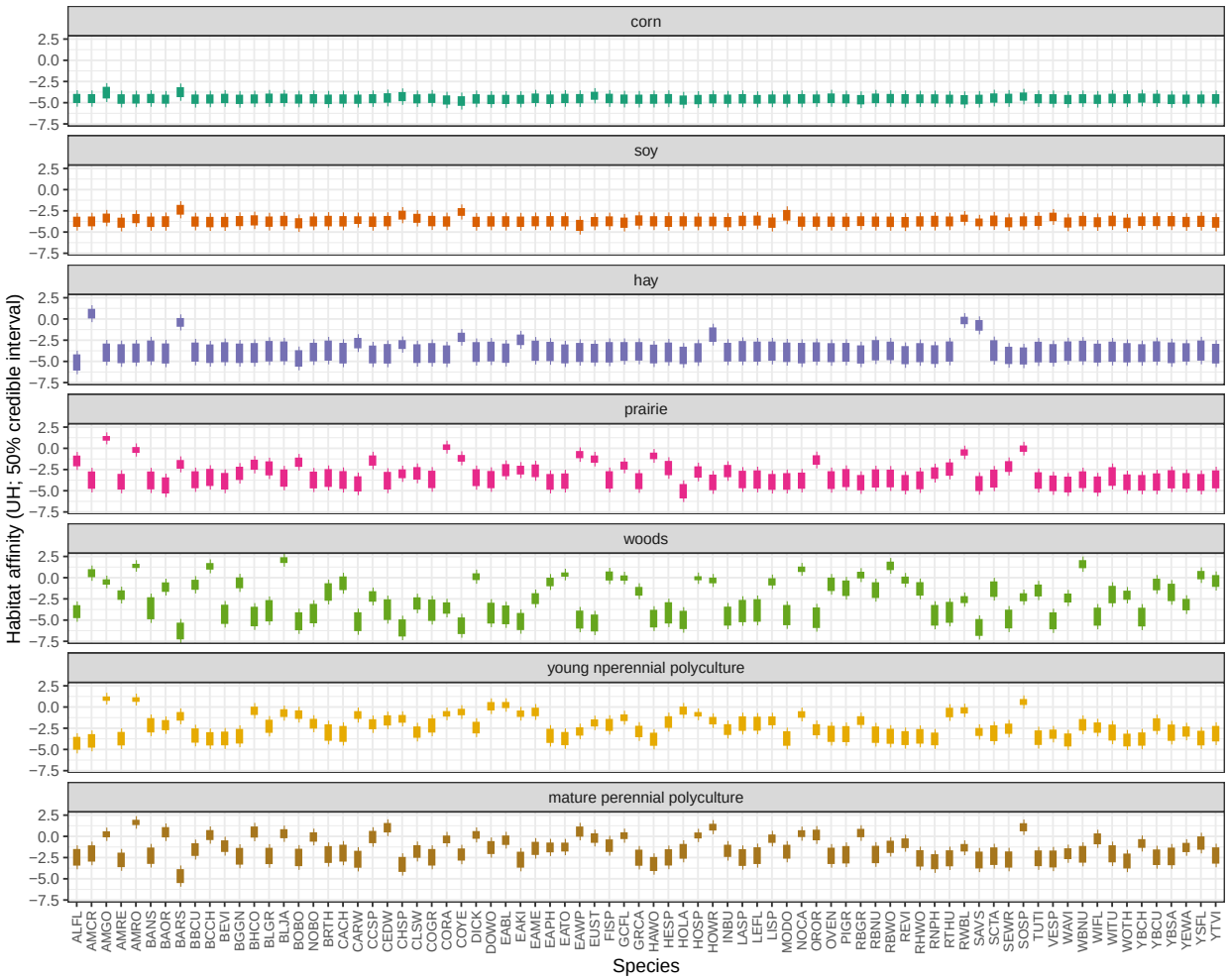

Figure S7: Model estimates of each species' habitat affinity. 50% credible interval is shown. Model accounts for non-detection bias. See Figure S6 for affinity faceted by species. See Table S2 for four-letter code legend.

(a)

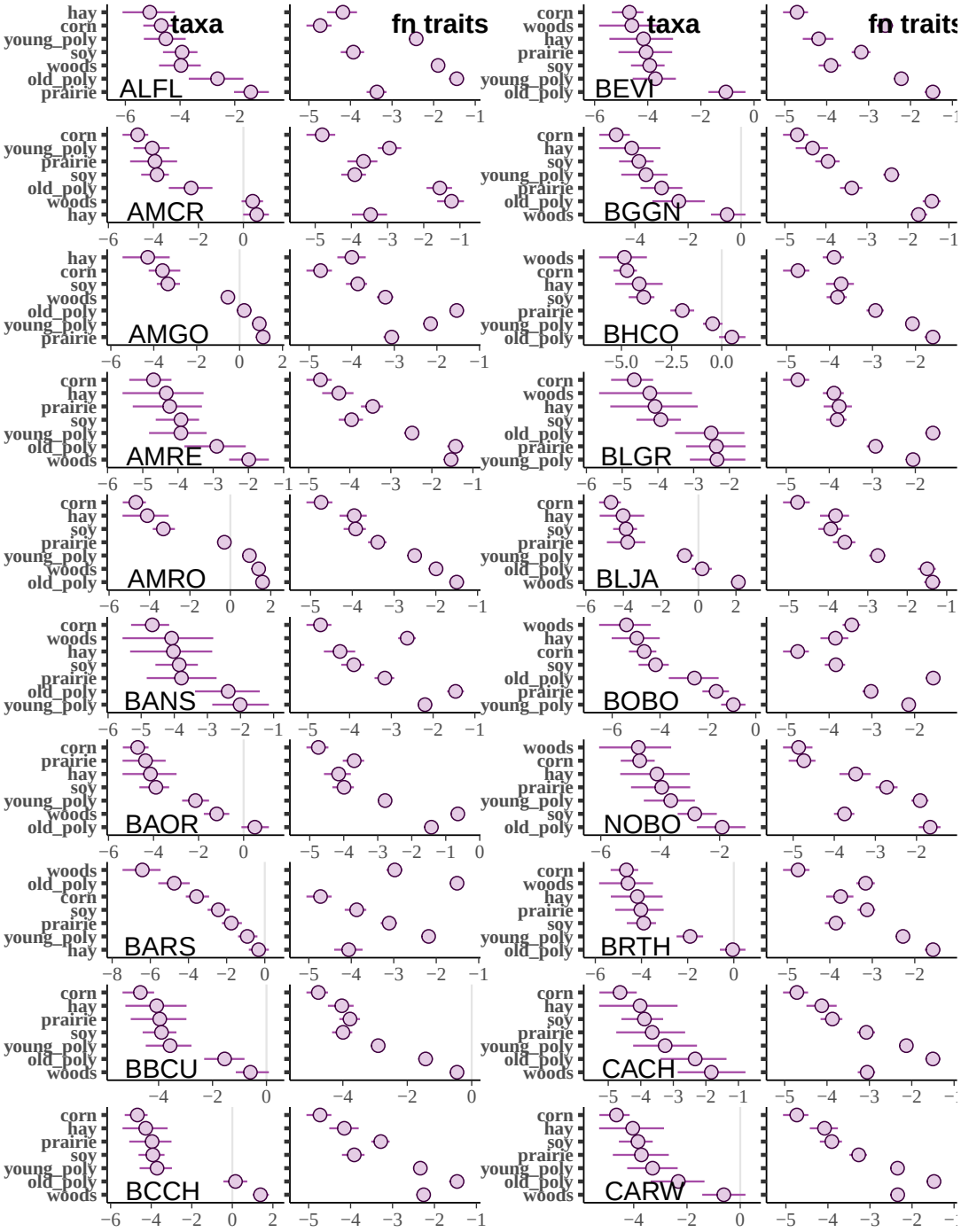
taxa
fn traits
ALFL
BEVI
AMCR
BGGN
AMGO
BHCO
AMRE
BLGR
AMRO
BLJA
BANS
BOBO
BAOR
NOBO
BARS
BRTH
BBCU
CACH
BCCH
CARW

(b)

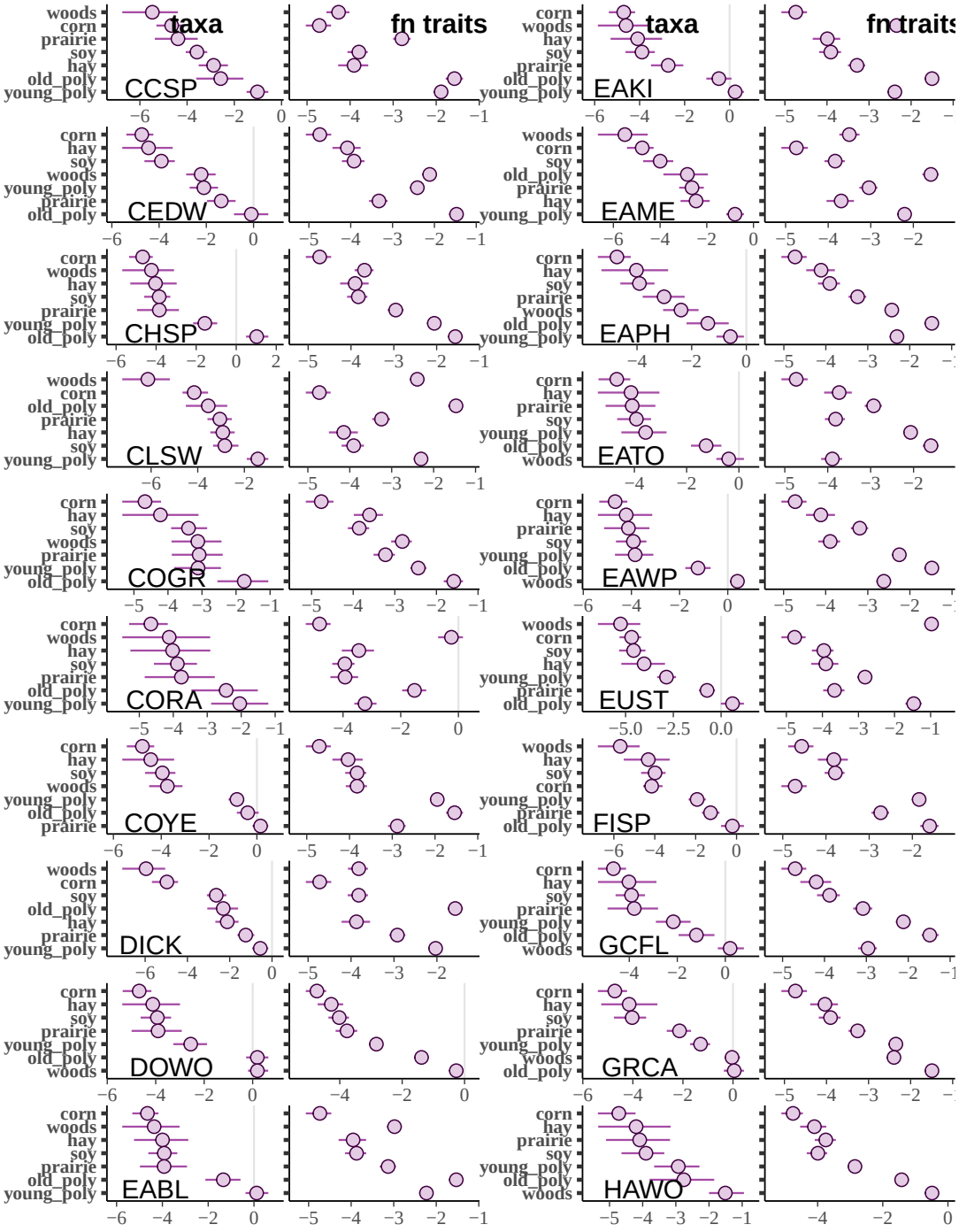
taxa
fn traits
CCSP
EAKI
CEDW
EAME
CHSP
EAPH
CLSW
EATO
COGR
EAWP
CORA
EUST
COYE
FISP
DICK
GCFL
DOWO
GRCA
EABL
HAWO

(c)

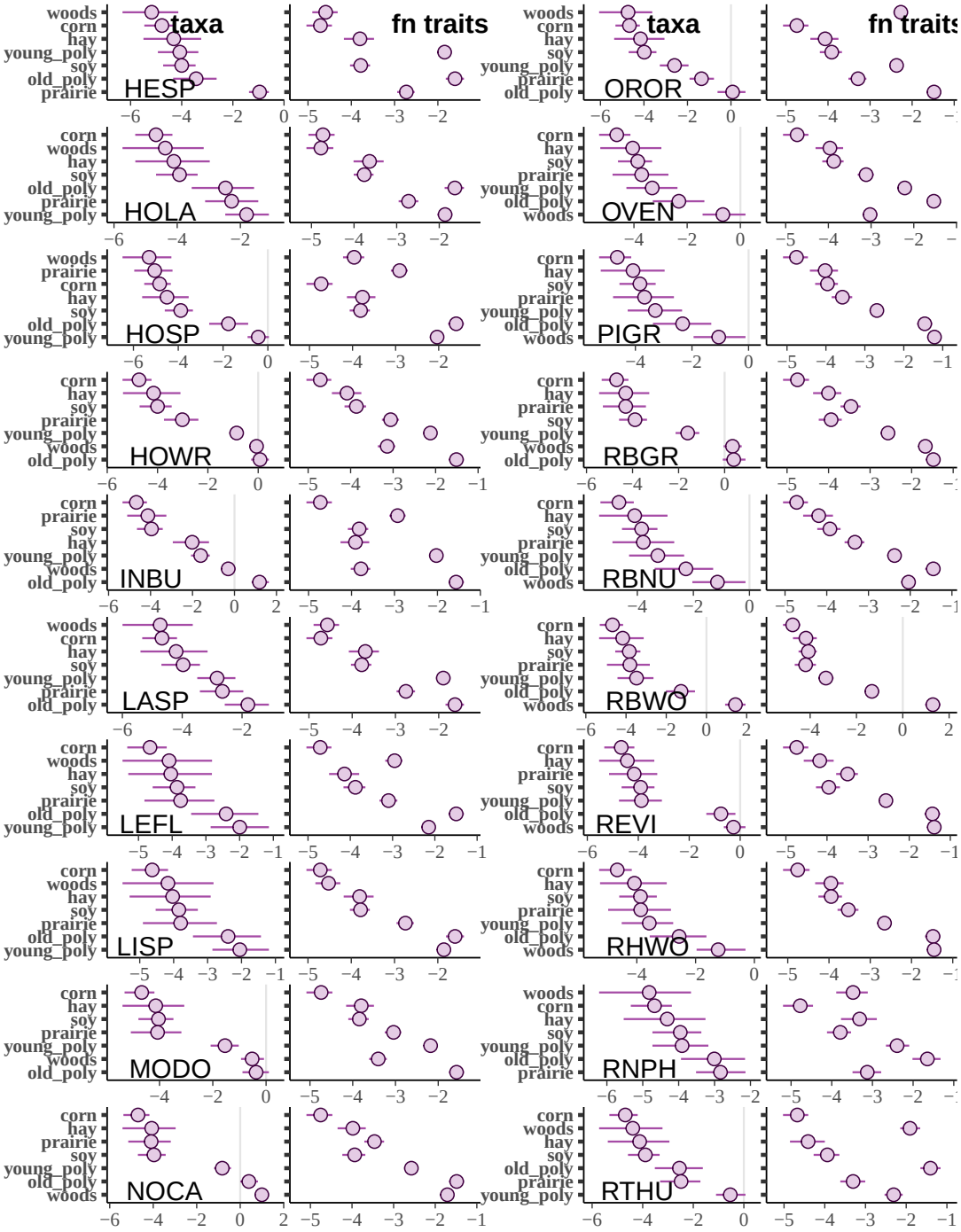
taxa
fn traits
HESP
ORORHOLA
OVENHOSP
PIGRHOWR
RBGRINBU
RBNULASP
RBWOLEFL
REVILISP
RHWOMODO
RNPHNOCA
RTHU

(d)

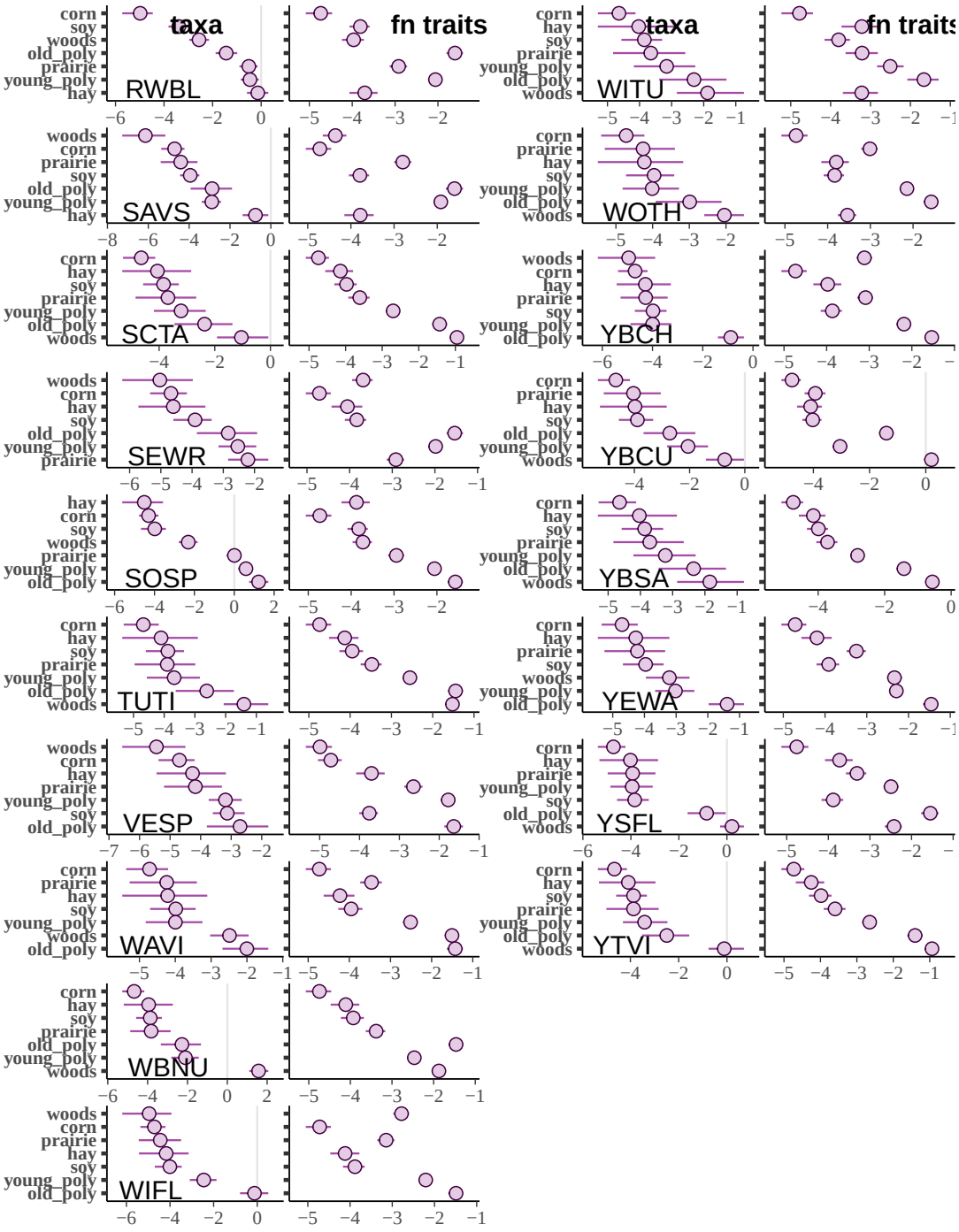

Figure S8: Model output for each taxa at each habitat type ('taxa') and the functional trait prediction ('fn trait'). Points represent medians and bars represent 50% credible intervals.

References

Betancourt, M., & Girolami, M. (2015). Hamiltonian Monte Carlo for hierarchical models. In S. K. Upadhyay, U. Singh, D. K. Dey, & A. Loganathan (Eds.), *Current trends in bayesian methodology with applications* (pp. 79–101). Chapman; Hall/CRC. https://doi.org/10.1201/b18502-5

Carpenter, B. (2016). The impact of reparameterization on point estimates. *Stan documentation case studies*.

Carpenter, B., Gelman, A., Hoffman, M. D., Lee, D., Goodrich, B., Betancourt, M., Brubaker, M., Guo, J., Li, P., & Riddell, A. (2017). Stan: A probabilistic programming language. *Journal of Statistical Software*, *76*(1). https://doi.org/10.18637/jss.v076.i01

Dennis, E. B., Morgan, B. J., & Ridout, M. S. (2015). Computational aspects of N-mixture models. *Biometrics*, *71*(1), 237–246. https://doi.org/10.1111/biom.12246

Hoffman, M. D., & Gelman, A. (2014). The No-U-Turn Sampler: adaptively setting path lengths in Hamiltonian Monte Carlo. *J. Mach. Learn. Res.*, *15*(1), 1593–1623.

Ingram, T., & Shurin, J. B. (2009). Trait-based assembly and phylogenetic structure in northeast Pacific rockfish assemblages. *Ecology*, *90*(9), 2444–2453. https://doi.org/10.1890/08-1841.1

Jetz, W., Sekercioglu, C. H., & Böhning-Gaese, K. (2008). The worldwide variation in avian clutch size across species and space. *PLoS Biology*, *6*(12), e303. https://doi.org/10.1371/journal.pbio.0060303

Kéry, M., Royle, J. A., & Schmid, H. (2005). Modeling avian abundance from replicated counts using binomial mixture models. *Ecological Applications*, *15*(4), 1450–1461.

Lê, S., Josse, J., & Husson, F. (2008). FactoMineR: A package for multivariate analysis. *Journal of Statistical Software*, *25*(1), 1–18. https://doi.org/10.18637/jss.v025.i01

Leibold, M. A., & Chase, J. M. (2017). *Metacommunity ecology*. Princeton University Press.

Lowther, P. E. (2020). Brown-headed cowbird (Molothrus ater), version 1.0. In A. F. Poole & F. B. Gill (Eds.), *Birds of the world*. Cornell Lab of Ornithology. https://doi.org/10.2173/bow.bnhcow.01

McElreath, R. (2020). *Statistical rethinking: A Bayesian course with examples in R and Stan* (2nd). CRC press.

Pillar, V. D., & d. S. Duarte, L. (2010). A framework for metacommunity analysis of phylogenetic structure. *Ecology Letters*, *13*(5), 587–596. https://doi.org/10.1111/j.1461-0248.2010.01456.x

Pillar, V. D., d. S. Duarte, L., Sosinski, E. E., & Joner, F. (2009). Discriminating trait-convergence and trait-divergence assembly patterns in ecological community gradients. *Journal of Vegetation Science*, *20*(2), 334–348. https://doi.org/10.1111/j.1654-1103.2009.05666.x

Pillar, V. D. (1999). The bootstrapped ordination re-examined. *Journal of Vegetation Science*, *10*(6), 895–902. https://doi.org/10.2307/3237314

Royle, J. A. (2004). N-mixture models for estimating population size from spatially replicated counts. *Biometrics*, *60*, 108–115.

Schönemann, P. H., & Carroll, R. M. (1970). Fitting one matrix to another under choice of a central dilation and a rigid motion. *Psychometrika*, *35*(2), 245–255.

Stubs, W. J., & Wilson, J. B. (2004). Evidence for limiting similarity in a sand dune community. *Journal of Ecology*, *92*(4), 557–567. https://doi.org/10.1111/j.0022-0477.2004.00898.x

Tobias, J. A., & Pigot, A. L. (2019). Integrating behaviour and ecology into global biodiversity conservation strategies. *Philosophical Transactions of the Royal Society B: Biological Sciences*, *374*(20190012). https://doi.org/10.1098/rstb.2019.0012